PHYSICAL REVIEW VOLUME 100, NUMBER 1 OCTOBER 1, 1955

Scattering of Positive Pions by Hydrogen at 189 Mev*

H. L. ANDERSON, W. C. DAVIDON, M. GLICKSMAN,† AND U. E. KRUSE
Institute for Nuclear Studies, The University of Chicago, Chicago, Illinois

(Received April 13, 1955)

The differential and total cross section of pions on hydrogen has been measured for 189 Mev positive pions. Liquid hydrogen was used as the scatterer; the incident and scattered pions were detected with scintillation counters. The angular distribution was fitted by: $\sigma=(7.24\pm0.76)+(3.1\pm1.3)\cos\chi+(25.6\pm2.6)\cos^2\chi$ millibarns per sterad. The total cross section measured by transmission was 194.1 ± 5.2 millibarns. A phase shift analysis was made using these results in conjunction with data obtained previously on the scattering of negative pions. The analysis was restricted to S and P waves and assumed conservation of isotopic spin. Four solutions were obtained. The one which is consistent with the requirements of causality and which corresponds to the preferred solution of de Hoffmann *et al.* is $\alpha_1=-2.8°\pm4.5°$, $\alpha_3=-11.3°\pm3.2°$, $\alpha_{11}=-2.6°\pm7.5°$, $\alpha_{13}=-2.1°\pm3.8°$, $\alpha_{31}=-11.6°\pm5.1°$, $\alpha_{33}=98.8°\pm3.6°$.

INTRODUCTION

THE scattering of pions with nucleons has been interpreted in terms of a set of phase shifts specifying the interaction in the possible states of the pion-nucleon system. In particular, the high-energy data have been analyzed by several authors,[1-3] and a preferred set of phase shifts has been proposed. This set has a resonance behavior for the state of isotopic spin $\frac{3}{2}$ and total angular momentum $\frac{3}{2}$. These analyses were based primarily on measurements of π^- differential cross sections, supplemented to some extent by some data on π^+ total cross sections. The present experiments were undertaken to complement the π^- scattering data at 191 Mev[4] with the corresponding π^+ data, and in this way improve the knowledge of the phase shifts at this energy. The present work extends that carried out at 165 Mev and reported in a companion paper.[5]

Due to the low intensity of positive pions available, a rather poor geometry was used. This necessitated special corrections in analyzing the data. The same corrections were used to reanalyze the previous negative pion data. A separate experiment to determine the efficiencies of the counters used in the charge exchange reactions led to a reanalysis of this reaction. All the results of counter measurements were then used as a basis for a new phase-shift analysis. The accuracy of the phase-shift solutions was also explored.

EXPERIMENTAL ARRANGEMENT

The experimental arrangement was essentially the same as that used in previous work from the laboratory.[6] A larger liquid hydrogen target of 6-inch diameter was used. Details of the geometry are shown in Fig. 1. Counters 1 and 2 were plastic scintillators $\frac{1}{8}$-inch thick and 2 inches$\times 2\frac{1}{16}$ inches. Counters 3, 4, 5, and 6 were 4-inch$\times$6-inch liquid scintillators described previously.[6] The use of four such counters made it possible to observe the scattered pions at two angles simultaneously.

Transmission measurements were made to obtain the total cross sections independently. Measurements were taken with the 4-inch$\times$6-inch counters set at 0°. In addition, 8-inch diameter liquid scintillation counters were used in the geometry of Fig. 2. A similar arrangement with the 8-inch counters was employed for range measurements in copper.

PION BEAMS

A beam of positive pions was obtained by bombarding a copper target in the cyclotron. Pions created in the backward direction emerged from the cyclotron and passed through a channel in the shielding to the experimental area. After passing through an analysing magnet and a proton filter of polyethylene, the pion flux was determined by counters 1 and 2. The flux available was roughly 300 pions/min. This was considerably greater than what could be obtained using a beryllium target.

The energy of the pions was determined from a range measurement in copper. The mean range corre-

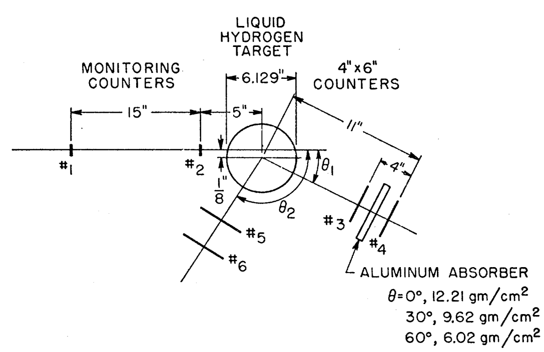

FIG. 1. Arrangement for observing the scattering of positive pions in hydrogen.

* Research supported by a joint program of the Office of Naval Research and the U. S. Atomic Energy Commission.
† Now at David Sarnoff Research Center, RCA Laboratories, Princeton, New Jersey.
[1] Fermi, Metropolis, and Alei, Phys. Rev. **95**, 158 (1954).
[2] de Hoffmann, Metropolis, Alei, and Bethe, Phys. Rev. **95**, 1586 (1954).
[3] R. L. Martin, Phys. Rev. **95**, 1606 (1954).
[4] M. Glicksman, Phys. Rev. **95**, 1045 (1954).
[5] H. L. Anderson and M. Glicksman, preceding paper [Phys. Rev. **100**, 268 (1955).
[6] Anderson, Fermi, Martin, and Nagle, Phys. Rev. **91**, 155 (1953).

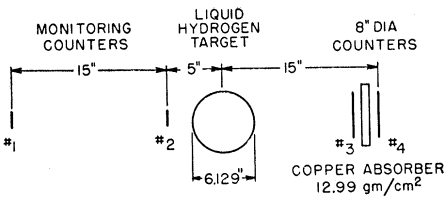

FIG. 2. Arrangement for making transmission measurements on positive pions in hydrogen.

sponded to 90.68 g/cm². Corrections for multiple scattering in the copper and counters and for energy loss in the target walls and counters gave a mean range at the center of the empty target of 97.33 g/cm². From the range curves of Aron[7] the corresponding energy of the pions at the center of the hydrogen filled target was 188.5 Mev. The effective energy spectrum had a full width at half maximum of 13.2 Mev. The fraction of muons in the beam was determined from the range curve; 2.2 percent of the beam were muons that had come through the analyzing magnet. A further 1.9 percent decayed in flight so as to be included by the monitoring counters. Thus 4.1 percent of the number of counts in counters 1 and 2 were due to muons.

In order to determine the distribution of the beam in the hydrogen target, the horizontal intensity distribution at the target position was measured directly with a scintillator $\frac{1}{4}$ inch wide and 2 inches high. The results were used to obtain the effective number of hydrogen scatterers and to correct for their finite extension.

ELASTIC SCATTERING OF POSITIVE PIONS

The differential cross section for the scattering of positive pions was measured at five angles. At 30° and 60°, aluminum absorbers were placed between the counters to eliminate all recoil protons. Measurements were taken simultaneously at two scattering angles, and with the target alternately filled with liquid hydrogen or containing only hydrogen gas at near liquid hydrogen temperature. These measurements are recorded as the ratio Q/D, quadruple coincidences divided by the double coincidences observed in the incident beam monitors. The simple differences in this ratio, Q/D, were taken as the effect of the additional hydrogen introduced. The results are given in Table I. The errors stated are those due to counting statistics only.

TABLE I. Measurement of elastic scattering of positive pions.

Lab angle	$10^4\,(Q/D)_{\mathrm{H}}$	$10^4\,(Q/D)_{\mathrm{No\,H}}$	$10^4\,(Q/D)_{\mathrm{net}}$
31.2°	45.0 ±1.33	10.9 ±0.93	34.1 ±1.6
60.9°	14.64±0.76	3.37±0.50	11.3 ±0.9
90.6°	14.54±0.74	5.86±0.54	8.68±0.9
120.3°	14.58±0.80	3.11±0.50	11.5 ±0.95
150.0°	21.54±0.92	4.69±0.59	16.9 ±1.6

[7] W. A. Aron, University of California Radiation Laboratory Report, UCRL-1325 (unpublished).

TRANSMISSION EXPERIMENTS

The total cross section was separately determined by transmission measurements. Two measurements were made using the 8-inch counters. A copper absorber of 12.99 g/cm² was used between counters 3 and 4 to discriminate against recoil protons. A third measurement was made with the 4-inch×6 inch counters, with an aluminum absorber of 12.21 g/cm².

Under the assumption that muons in the beam do not interact, the cross section is given by

$$\sigma = -\frac{1}{N}\ln\left[R - \frac{r}{T}(1-R)\right].$$

R is $(Q/D)_{\mathrm{H}}/(Q/D)_{\mathrm{No\,H}}$, where N is the number of hydrogen atoms/cm², r is the ratio of muons to pions at the center of the target, and T is the fraction of pions at the center of the target which are detected in counters 3 and 4 (regardless of whether or not they decay on the way). Q/D measures the cross section for scattering greater than θ_{max}, the half-angle subtended by counter 4 at the center of the target. The total cross section is obtained by adding the cross section up to θ_{max}; this was estimated from the angular distribution measurements. The final results are in Table II.

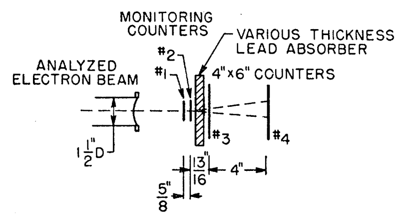

FIG. 3. Arrangement for measuring electron detection efficiencies of counters used in charge-exchange measurements.

The weighted mean of all the transmission measurements was 194.1±5.2 mb, including a two percent error in the value of N.

GAMMA EFFICIENCIES

A measurement was made to determine the energy dependence of the gamma efficiencies of the counter arrangement used in the earlier charge exchange scattering experiment.[4] The efficiencies for the detection of pairs produced at different depths in the lead radiator were derived from measurements on the transmission of electrons of different energies through various thicknesses of lead. These results were then combined with known pair production cross sections[8,9] to give the gamma efficiencies of the counters. The experimental arrangement used is shown in Fig. 3.

The dimensions and relative positions of the lead and counters 3 and 4 were the same as in the charge exchange measurement. Counters 1 and 2 were $\frac{1}{2}$-inch ×$\frac{1}{2}$-inch plastic scintillators and served to define and

[8] De Wire, Ashkin, and Beach, Phys. Rev. **83**, 505 (1951).
[9] J. L. Lawson, Phys. Rev. **75**, 433 (1949).

TABLE II. Measurement for the total cross section of positive pions.

Counter No. 3 and No. 4	θ_{max}	Absorber	$R=\frac{(Q/D)_H}{(Q/D)_{No\ H}}$	γ/T	$\sigma_T-\int_0^{\theta_{max}} d\Omega\frac{d\sigma}{d\Omega}$	$\int_0^{\theta_{max}} d\Omega\frac{d\sigma}{d\Omega}$	σ_T
8 in.	15.2°	12.99 g/cm² Cu	0.9038±0.0051	0.052±0.01	167.2±9.1 mb	12.1±2.5 mb	179.3±9.4 mb
8 in.	15.2°	12.99 g/cm² Cu	0.8945±0.0024	0.052±0.01	184.3±4.5 mb	12.1±2.5 mb	196.4±5.2 mb
4 in.×6 in.	14.1°[a]	12.21 g/cm² Al	0.8924±0.0023	0.053±0.01	188.4±4.4 mb	10.5±3.0 mb	196.5±5.3 mb

[a] Angle for circular counter of area equal to 4 in.×6 in.

monitor the incident beam. Wire measurements were used to determine the electron energies, which ranged from 10 to 75 Mev. At each energy the ratio of triple coincidences in counters 1, 2, and 3, to the double coincidences in 1 and 2, gave the fraction of incident electrons which traversed the lead. The quadruples to triples rate, gave the fraction which was not scattered out of the No. 4 counter. The results are summarized in Table III.

To obtain the gamma efficiencies of the counters, the probability was determined for a photon to traverse various thicknesses of lead, produce a pair, and have at least one of the pair detected. Numerical integrations were made over the counter dimensions, lead thickness, and energy division of the pair produced. The average efficiencies for gammas produced anywhere in the target are presented in Fig. 4. The dependence on the angle at which the detector was set was small and was neglected here.

TABLE III. Measurement of attenuation and scattering of electron beams in lead.

Lead (g/cm²)	Energy (Mev)	T/D	Q/T Position[a] 1	2	3	4
0	8.7	0.98	0.88	0.45	0.77	0.34
	18.2	0.98	0.93	0.62	0.88	0.47
	37.2	0.99	0.98	0.68	0.97	0.69
	56.2	0.99	0.98	0.78	0.99	0.75
	75.2	0.99	0.97	0.81	0.97	0.75
2.76	8.7	0.17	0.24	0.088	0.076	0.065
	18.2	0.70	0.36	0.26	0.29	0.28
	37.2	0.90	0.71	0.46	0.66	0.42
	56.2	0.93	0.86	0.53	0.73	0.45
	75.2	0.93	0.88	0.59	0.86	0.61
5.55	8.7	0.00	...	...	...	...
	18.2	0.22	0.17	0.16	0.19	0.11
	37.2	0.67	0.45	0.31	0.45	0.34
	56.2	0.81	0.61	0.42	0.56	0.36
	75.2	0.89	0.71	0.44	0.57	0.41
7.41	8.7	0.00	...	...	...	...
	18.2	0.15	0.19	0.14	0.23	0.00
	37.2	0.50	0.46	0.27	0.34	0.15
	56.2	0.69	0.52	0.42	0.46	0.29
	75.2	0.78	0.65	0.53	0.61	0.31

[a] Position of beam on first 4 in.×6 in. counter (No. 3).
1. Center.
2. 2 in. from center along 6 in. axis.
3. 1½ in. from center along 4 in. axis.
4. 2 in. from center along 6 in. axis and 1½ in. from center along 4 in. axis.

Calculations were also made in which the Monte Carlo results of Wilson[10,11] were used for the electron scattering. These gave smaller efficiencies as shown in Fig. 4. The uncertainties involved in deducing these efficiences were such that we assigned an error of 15 percent and included this in all the errors stated.

The experimental determination of the gamma efficiency was subject to two tests. First, using the computed results, a determination was made of the efficiency to be expected in a measurement of the Panofsky effect. The results of this calculation gave 54.3±8.1 percent as compared to 58±6 percent obtained directly in a previous measurement.[6] The other test was a comparison between the total cross section for π^- and the sum of integrated differential cross sections for $\pi^-\to\pi^-$, $\pi^-\to\pi^0$, and $\pi^-\to\gamma$. The total cross section was (63.5±1.6 mb) whereas the sum of integrated cross sections was 68.0±3.5 mb. The difference is not outside the experimental error in both cases.

DATA ANALYSIS

Elastic Scattering

The data analysis of the elastic scattering experiment was complicated by the poor geometries used to obtain reasonable counting rates with the weak incident beam. Thus, a number of corrections were needed to

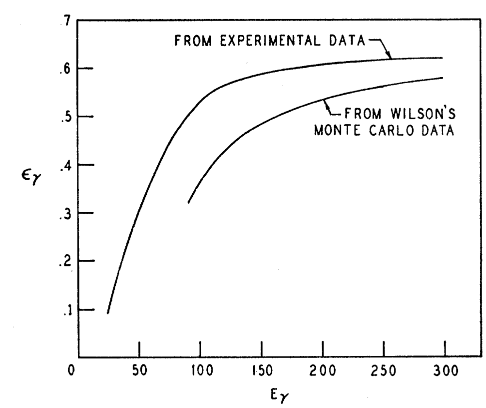

FIG. 4. Gamma detection efficiencies of counters used in charge exchange measurements. E_γ is the gamma energy, ϵ_γ the detection efficiency.

[10] R. R. Wilson, Phys. Rev. 84, 100 (1951).
[11] R. R. Wilson, Phys. Rev. 86, 261 (1952).

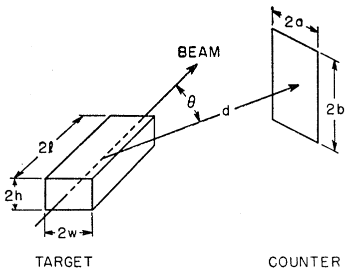

FIG. 5. Idealized target and counter geometry used as basis for geometry corrections.

obtain the scattering cross section from the experimental data. Accordingly, corrections were made for the finite range of scattering angles allowed by the detector and target, each angle being weighted by its own solid angle. Further corrections for thick targets were made to take into account the attenuation of the incident and scattered beams in the target and the multiple scattering in the target. Besides these, the usual corrections for efficiencies of the counters and muon contamination of the beam were made. The cross section for poor geometries was, therefore, taken to be

$$\frac{d\sigma}{d\Omega}=\left(\frac{Q}{D}\right)_{\text{net}}\frac{1}{N\Omega}\frac{1}{f\epsilon GM},$$

where $(Q/D)_{\text{net}}$ as above represents the net quadruples rate, H-liquid minus H-gas, divided by the doubles rate of the incident beam monitor. The mean number of hydrogen scatterers/cm^2 seen by the actual beam distribution is N; Ω is the solid angle of the fourth counter averaged over the target; f is the fraction of the doubles counts which actually correspond to pions at the center of the target, omitting however possible attenuation in the hydrogen. Thus, fD is the number of pions at the center of the target with no hydrogen in the target; ϵ is the efficiency of counting pions which are scattered toward the counters. This efficiency takes into account nuclear absorption in the third counter and in the absorber between the third and fourth counters together with possible inefficiencies in the counters. G represents the geometrical corrections necessary because of the finite range of scattering angles observed in the detector. Finally, M is the correction for multiple scattering in the target and attenuation in the hydrogen of the incident and scattered beams.

The quantity N was determined from the beam scan together with the dimensions of the target and difference in density of liquid hydrogen and hydrogen gas. The mean path length was 5.96 inches and the net density, 0.070 g/cm^2, therefore $N=6.39\times10^{23}$ atoms/cm^2. The uncertainty in N was estimated to be two percent. The quantity f was 0.947 as determined from the muon contamination of 4.1 percent, obtained from the range curve, and the 1.2 percent absorption of pions in the second counter and front target wall. The accuracy of f was estimated to be ±1 percent.

TABLE IV. Factors in analysis of π^+ scattering.

Lab angle (degree)	N	f	ϵ	M	Ω	G
31.2	6.39×10^{23}	0.947	0.854	0.932	0.1936	0.934
60.9			0.891	0.974	0.1792	1.054
90.6			0.962	0.974	0.1728	1.048
120.3			0.962	0.954	0.1796	0.982
150.0			0.962	0.965	0.1936	0.987

The correction M for attenuation and multiple scattering took into account the energy and angular dependence of the scattering cross section. However, the following approximations were made to obtain a simple formula. The scattering volume was assumed to be spherical, and all the first scatterings were assumed to occur at the center of this sphere. Only double scatterings were considered and these were taken to occur as the particle left the center of the sphere. Attenuations were assumed to occur on the way into the center and on the way out from the center. With these assumptions the single scattering s per unit solid angle is given by

$$\frac{s}{fD\Omega}=e^{-\frac{1}{2}N\sigma_T(0)}N\sigma(\theta)e^{-\frac{1}{2}N\sigma_T(\theta)}$$
$$=N\sigma(\theta)\{1-\tfrac{1}{2}N[\sigma_T(0)+\sigma_T(\theta)]\},$$

to first order in $N\sigma$. Here $\sigma(\theta)$ is the differential cross section for scattering into θ, $E(\theta)$ is the energy of the meson scattered into the angle θ and $\sigma_T(\theta)$ is the total cross section for pion scattering at this energy. The ratio of double scattering to single scattering into a counter at angle θ is given by

$$\frac{d}{s}=\frac{N}{2\sigma_1(\theta)}\int d\phi d(\cos\alpha)\sigma_2(\chi)\sigma_1(\alpha,\phi),$$

where α and ϕ are the polar and azimuthal angles of the first scattering given by $\sigma_1(\alpha,\phi)$. The plane formed by the incident beam and the center of the counter is taken as $\phi=0$. The cross section for second scattering is $\sigma_2(\chi)$ where χ is the angle between the initial scattering and the direction of the counter at θ. To obtain an integrable form, the laboratory differential cross section for second scattering, $\sigma_2(\chi)$ was expanded in terms of Legendre polynomials; the coefficients in the expansion depend on the energy of the pion after the first scattering and hence on α. Thus,

$$\sigma_2(\chi)=\sum a_l(\alpha)P_l(\chi).$$

With the use of the addition theorem for spherical harmonics,

$$P_l(\chi)=\frac{4\pi}{2l+1}\sum_{m=-l}^{l}\gamma_l^{m*}(\alpha,\varphi)\gamma_l^m(\theta,0),$$

and after an integration over ϕ, the ratio of double to

TABLE V. Estimated standard errors in π^+ cross section.

Lab angle (degree) \ Quantity	N,ϵ,t %	M %	Ω %	G %	$\Delta\theta$ %	ΔE %	Subtotal %	Subtotal mb	Statistical mb	Total estimate mb
31.2	3.0	3.9	2.3	1.1	2.0	2.1	6.2	2.4	1.8	3.0
60.9	3.0	1.3	2.5	2.2	2.5	1.1	5.4	0.62	0.9	1.06
90.6	3.0	1.3	2.7	1.2	0.5	0.7	4.5	0.38	0.9	0.98
120.3	3.0	2.3	2.5	0.9	0.8	0.3	4.7	0.55	1.0	1.4
150.0	3.0	1.9	2.3	0.2	0.3	0.1	4.2	0.66	1.5	1.64

single scattering becomes

$$\frac{d}{s}=\frac{\pi N}{\sigma_1(\theta)}\sum_l P_l(\theta)\int_{-1}^{+1} dt a_l(t)\sigma_1(t)P_l(t),$$

where $t=\cos\alpha$. The coefficients $a_l(t)$ were evaluated from the scattering data at lower energies, terms up to $l=2$ only were included. Therefore

$$(s+d)/fD\Omega=N\sigma_1(\theta)[1-\tfrac{1}{2}N\sigma_T(0)-\tfrac{1}{2}N\sigma_T(\theta)+(d/s)]$$

and the correction M to the cross section because of attenuation and double scattering in the target is

$$M=1-\tfrac{1}{2}N\sigma_T(0)-\tfrac{1}{2}N\sigma_T(\theta)+(d/s).$$

The uncertainties in M vary with the scattering angle, from four percent at 31.2° to 1.9 percent at 150°.

The geometrical corrections appear in terms of the two quantities Ω, the corrected solid angle, and G a correction factor for the variations of the cross section over the range of angles detected at one counter setting. If $\sigma(\phi)$ represents the true scattering cross section in the laboratory system, then for a counter at θ,

$$\frac{(Q/D)_{\text{net}}(\theta)}{\epsilon fNM}=\frac{1}{V}\int\int_A d\tau da\sigma(\phi)\frac{\cos\delta}{r^2},$$

where $d\tau$ is an element of the target volume V, da is an element of the counter area A, and $\mathbf{r}$ is a vector connecting $d\tau$ with da. The angle between $\mathbf{r}$ and the direction of the incident beam is ϕ, and δ is the angle between $\mathbf{r}$ and the normal to the counter.

Let the counter be of width $2a$ and height $2b$ centered at a scattering angle θ a distance d from the center of the target of width $2w$, height $2h$, and length $2l$ as in Fig. 5. When $\sigma(\phi)$ is expanded in a Taylor series about θ, then in terms of

$$(d\sigma/d\phi)|_\theta=\sigma'(\theta) \quad\text{and}\quad (d^2\sigma/d\phi^2)|_\theta=\sigma''(\theta),$$

$$\frac{\left(\frac{Q}{D}\right)_{\text{net}}(\theta)}{\epsilon fNM}=\frac{A}{d^2}[\sigma(\theta)(1+\alpha)+\beta\sigma'(\theta)+\tfrac{1}{2}\gamma\sigma''(\theta)].$$

To second order in a/d, b/d, etc., α, β, and γ are

$$\alpha=\frac{1}{d^2}\left[-\frac{a^2}{2}-\frac{b^2}{2}-\frac{h^2}{2}+\frac{l^2}{2}(3\cos^2\theta-1)+\frac{w^2}{2}(3\cos^2\theta-1)\right]$$

$$\beta=\frac{1}{d^2}\left[\frac{b^2}{6}\cot\theta+\frac{h^2}{6}\cot\theta+l^2\cos\theta\sin\theta-w^2\cos\theta\sin\theta\right]$$

$$\gamma=\frac{1}{d^2}\left[\frac{a^2}{3}+\frac{l^2}{3}\sin^2\theta+\frac{w^2}{3}\cos^2\theta\right].$$

The higher order terms cannot be neglected for small θ.

If the dependence on σ' and σ'' is included in a factor G, then

$$\frac{\left(\frac{Q}{D}\right)_{\text{net}}(\theta)}{\epsilon fNM}=\frac{A}{d^2}\sigma(\theta)(1+\alpha)G,$$

with

$$G=1+\beta\sigma'(\theta)+\tfrac{1}{2}\gamma\sigma''(\theta).$$

A further small correction is made for scattering angles near 90°. For these angles, the extremities of the target do not see all of the fourth counter, a fraction λ is cut off by the third counter. The final value for Ω therefore is

$$(A/d^2)(1+\alpha)(1-\lambda).$$

The uncertainty in Ω is estimated at two percent and in G as two percent.

The values of the various quantities for the 189 Mev positive pion scattering are given in Table IV.

In addition to the uncertainties in the various constants of Table IV, the uncertainty in the angle is estimated as ±0.7° and the uncertainty in the energy, estimated as ±2 Mev, can contribute to the uncertainties in the final cross sections. The estimated standard errors in each cross section are given in Table V, divided

TABLE VI. Cross section for π^+ scattering.

Lab angle (degree)	C. M. angle	$10^4\ (Q/D)_{\text{net}}$	$(d\sigma/d\Omega)_{\text{lab}}$ in mb	$(d\sigma/d\omega)_{\text{c.m.}}$ in mb
31.2	40.3	34.1±1.8	39.2±3.0	25.0±1.9
60.9	75.7	11.3±0.9	11.4±1.1	9.2±0.8
90.6	106.6	8.7±0.9	8.5±1.0	9.1±1.0
120.3	133.4	11.5±1.0	11.7±1.1	16.4±1.6
150.0	157.1	16.9±1.6	15.8±1.6	26.6±2.8

TABLE VII. Factors in analysis of elastic π^- scattering.

Lab angle	N	f	ϵ	M	Ω	G	$\overline{\epsilon_\gamma}$
25.7	3.59×10^{23}	0.97	0.858	0.975	0.112	0.974	0.025
51.4			0.938	0.985	0.111	0.991	0.025
77.1			0.968	0.986	0.109	1.040	0.024
102.8			0.968	0.987	0.109	1.009	0.024
128.6			0.968	0.987	0.111	1.004	0.024
154.3			0.968	0.988	0.112	1.003	0.024

into contributions from statistics and all other sources. The errors estimated were combined quadratically to give the over-all error estimate. The final cross sections are then given in Table VI.

The elastic negative pion experiments previously performed[4] were reanalyzed in the same way as the positive pion experiments. In this experiment, part of the counting rate is due to gamma rays from the charge exchange reaction. Therefore

$$\sigma_{\pi^-}=\left[\left(\frac{Q}{D}\right)^- -\frac{\epsilon_\gamma^-}{\epsilon_\gamma^0}\left(\frac{Q}{D}\right)^0_{\text{net}}\right]\frac{1}{N\epsilon fGM\Omega},$$

where ϵ_γ^- and ϵ_γ^0 are the average efficiencies for γ detection in the elastic scattering and charge exchange measurements; $(Q/D)_{\text{net}}^-$ and $(Q/D)_{\text{net}}^0$ are the net quadruples to doubles observed in the two arrangements. The quantity $\epsilon_\gamma^-/\epsilon_\gamma^0$ is roughly 4.5 percent.

The numerical values of the terms are given in Table VII, $(Q/D)^0_{\text{net}}$ is given in Table IX.

The cross sections are given in Table VIII and differ only slightly from the previous results.

The charge exchange scattering previously determined was also reanalyzed in terms of the efficiencies given in the section on gamma efficiencies. The analysis is the same as the one given by Bodansky, Sachs, and Steinberger.[12] and in the companion paper.[5]

The number of γ-ray counts due to the charge exchange reaction is converted to the center-of-mass system. The resulting number of counts per unit solid angle and per incident π^- is

$$n_\gamma=\frac{(Q/D)_{\text{net}}^0}{Nf\Omega}\frac{\Delta\Omega}{\Delta\omega}-n'.$$

TABLE VIII. Cross sections for elastic π^- scattering.

Lab angle	C. M. angle	$10^6\ (Q/D)_{\text{net}}$	$(d\sigma/d\Omega)\gamma$	$(d\sigma/d\Omega)_{\text{lab}}$	$(d\sigma/d\omega)_{\text{c.m.}}$
25.7	33.3	207.5 ± 19.9	13.19 ± 0.82	6.11 ± 0.68	3.85 ± 0.42
51.4	64.7	72.6 ± 8.8	7.56 ± 0.53	1.85 ± 0.26	1.38 ± 0.20
77.1	93.0	38.6 ± 6.4	5.02 ± 0.52	0.90 ± 0.18	0.85 ± 0.17
102.8	118.0	48.8 ± 6.5	5.73 ± 0.52	1.20 ± 0.19	1.45 ± 0.23
128.6	140.3	58.7 ± 7.0	5.66 ± 0.52	1.44 ± 0.20	2.14 ± 0.30
154.3	160.7	74.9 ± 9.4	6.13 ± 0.69	1.86 ± 0.26	3.16 ± 0.45

[12] Bodansky, Sachs, and Steinberger, Phys. Rev. **93**, 1367 (1954).

TABLE IX. Factors in analysis of π^- charge exchange scattering.

θ	χ	$(Q/D)_{\text{net}}$	N	f	Ω	n'	n_γ
25.7	32.3	285.6 ± 16.6	3.59×10^{23}	0.97	0.107	0.03	4.93 ± 0.79
57.4	62.8	157.0 ± 10.4			0.107	0.03	3.23 ± 0.53
77.1	90.7	99.4 ± 10.1			0.106	0.03	2.53 ± 0.45
102.8	115.6	109.4 ± 9.8			0.106	0.03	3.45 ± 0.60
128.6	138.4	106.0 ± 9.6			0.107	0.03	3.93 ± 0.69
154.3	159.6	115.1 ± 12.8			0.107	0.03	4.77 ± 0.88

$\Delta\Omega/\Delta\omega$ is the ratio of solid angles in the laboratory and center of mass systems and n' is the corresponding number of counts due to the reaction $\pi^-+p\rightarrow n+\gamma$.

Table IX gives the experimental results for n_γ. The 15 percent uncertainty for the efficiencies has been added to the statistical uncertainties.

With the π^0 distribution $\sum a_lP_l$ we have for n_γ

$$n_\gamma=\sum k_l\bar{\epsilon}_la_lP_l.$$

The values of $\bar{\epsilon}_l$ are given in Table X. For this energy, $k_0=2$, $k_1=1.414$, and $k_2=0.937$.

Figure 6 is a plot of the differential cross sections. For $\pi^-+p\rightarrow\pi^0+n$, the effective γ ray cross section n_γ/ϵ_0 is plotted. The curves represent the cross sections calculated from the first phase-shift solution. The cross sections for positive pion scattering determined by Homa, Goldhaber, and Lederman[13] are in rough agreement with the present measurements.

LEAST SQUARES FIT AND PHASE-SHIFT ANALYSIS

In order to provide a summary of the angular distribution measurements, to integrate the angular distributions, and to prepare an Ashkin diagram,[14] a least squares fit was made to the differential cross section by expressions of the form $a+b\cos\chi+c\cos^2\chi$.

In this least squares fit, and in the determination of the phase shifts, the quantity $M=\sum_i(\Delta_i/\epsilon_i)^2$ is minimized. The quantity Δ_i is the difference between the calculated and experimental cross sections, and ϵ_i is the experimental standard deviation. In the vicinity of the best fit, we consider M to depend quadratically on the parameters. This is exact in the case of the a, b, and c's. For the phase shifts, a fit was made to the actual dependence on M by a function of this type. Under these conditions, if the parameters are changed from

TABLE X. Efficiencies and coefficients in π^- charge exchange scattering.

C. M. angle χ	$\bar{\epsilon}_0$	$\bar{\epsilon}_1$	$\bar{\epsilon}_2$
32.3	0.57	0.60	0.63
62.8	0.53	0.59	0.63
90.7	0.51	0.58	0.63
115.6	0.48	0.57	0.62
138.4	0.47	0.56	0.62
159.6	0.45	0.55	0.62

[13] Homa, Goldhaber, and Lederman, Phys. Rev. **93**, 554 (1954).
[14] J. Ashkin and S. H. Vosko, Phys. Rev. **91**, 1248 (1953).

TABLE XI. Summary of least squares fit at 189 Mev.

Scattering process	Coefficients in fit: $d\sigma/d\omega=a+b\cos\chi+c\cos^2\chi$ (mb/sterad) a	b	c	$4\pi(a+c/3)$ (mb) σ_T		Error matrix G^{-1} (mb/sterad)^2 a	b	c	M_0
$\pi^+\rightarrow\pi^+$	7.24±0.76	3.1 ±1.3	25.6 ±2.6	198.3±8.5	a	0.5775	−0.1362	− 1.297	0.869
					b		1.7853	0.9993	
					c			6.689	
$\pi^-\rightarrow\pi^-$	0.79±0.14	0.26±0.22	3.10±0.42	23.0±1.4	a	1.904	−0.7784	− 4.065	2.46
					b		5.028	3.936	
					c			17.81	
$\pi^-\rightarrow\pi^0$	1.91±0.53	−0.33±0.60	5.1 ±1.6	45.3±3.2	a	0.2834	−0.0417	− 0.7274	0.78
					b		0.3600	0.1529	
					c			2.408	

their best values by x_i, then

$$M=M_0+\sum_{ij}x_ix_jG_{ij}.$$

G is a real, symmetric matrix with positive eigenvalues. The errors in the experimentally determined differential and total cross sections are assumed to be independent and normally distributed. This neglects the correlations introduced by such common factors as N, the number of hydrogen atoms per unit area, and also assigns a normal distribution to the systematic errors. With these assumptions, the probability for having obtained the experimental results when any set of x_i are chosen for the parameters is proportional to $e^{-M/2}$. The accuracy with which the parameters have been determined can then be expressed by the error matrix, G^{-1}, with the property

$$(G^{-1})_{ij}=\langle x_ix_j\rangle=\frac{\int dx_1\cdots dx_n e^{-M/2}x_ix_j}{\int dx_1\cdots dx_n e^{-M/2}}.$$

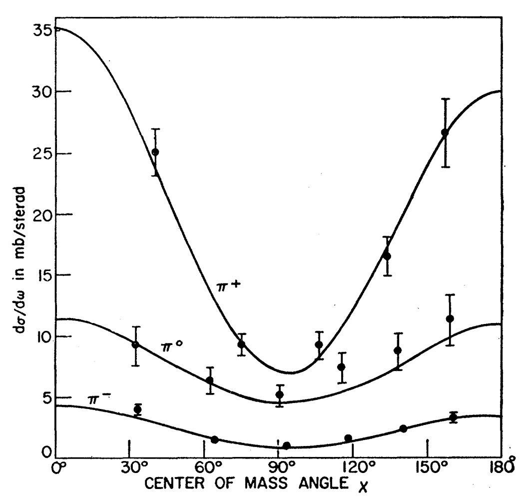

FIG. 6. Differential cross sections for elastic and charge-exchange scattering of 189-Mev pions by hydrogen. The curves correspond to the phase-shift solution 1.

The square root of the diagonal elements of G^{-1} gives the standard deviations for each of the parameters. The off-diagonal elements are the product of the correlation coefficients with the two corresponding standard deviations.

The results of the least squares fit of the form $a+b\cos\chi+c\cos^2\chi$ appear in Table XI, together with the integrated differential cross section, $\sigma_T=4\pi(a+c/3)$. The errors stated on a, b, and c are the roots of the diagonal elements of G^{-1}. The errors on σ_T include the effects of the negative correlation between a and c.

A phase-shift analysis of the data was carried out in the manner described in the earlier work from this laboratory.[5,6] The cross sections were expressed in terms of six phase shifts, assuming conservation of isotopic spin and limiting the analysis to S and P waves. The AVIDAC at the Argonne National Laboratory was used to seek the phase shifts giving the best fit to the transmission as well as angular distribution measurements.

Figure 7 shows the initial values of the phase shifts obtained from the Ashkin diagrams together with the final values obtained by the AVIDAC.

The twelve initial sets of phase shifts converged to four distinct types. The first and third were of the Fermi type ($\alpha_{33}>\alpha_{31}$), with the α_3 of the first greater

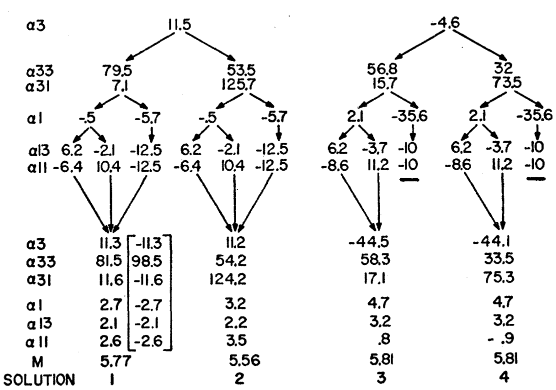

FIG. 7. Phase-shift solutions from Ashkin's diagram together with final values obtained with the AVIDAC.

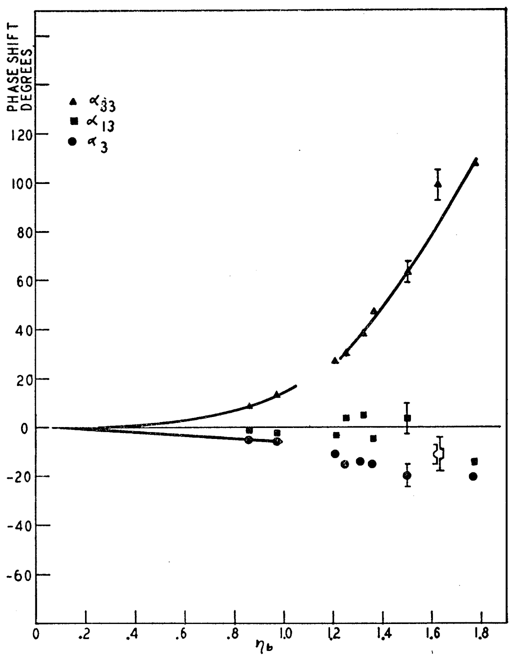

FIG. 8. Dependence of the phase shifts, α_{33}, α_{13}, and α_3 on η_b, the center of mass pion momentum in units of μc.

than that for the third. The second and fourth are the corresponding Yang types. The significance of these results is discussed in the next section.

To determine the accuracy with which the phase shifts were determined, G^{-1} was evaluated using the AVIDAC. Since the region in which $M=M_0+1$ is the most significant in the integrals involving $e^{-M/2}$, G^{-1} was determined by fitting an ellipsoid to the surface $M=M_0+1$ in the phase angle space. All the angles were varied individually and in pairs until a value of $M=M_0+1$ was reached. With the notation $S_{i+}(S_{i-})$ equal to the increase (decrease) in α_i necessary to change M by one, G_{ii} was evaluated from

$$G_{ii}=4/(S_{i+}+S_{i-})^2.$$

For the off-diagonal elements, pairs of angles were varied. The magnitude of the variation was always the same for each of the pairs, but all combinations of signs were used. With $S_{i+,\,j+}$, $S_{i+,\,j-}$, $S_{i-,\,j+}$, $S_{i-,\,j-}$ representing the magnitude of the change in each the angles i and j with the signs indicated, then G_{ij} was obtained from

$$G_{ij}=\frac{1}{(S_{i+,\,j+}+S_{i-,\,j-})^2}-\frac{1}{(S_{i+,\,j-}+S_{i-,\,j+})^2}.$$

This method for determining G gives an exact result if the surface $M=M_0+1$ is truly an ellipse centered at the nominal minimum. G is not affected to first order by a small displacement of the ellipse in any direction. The elements of the error matrix, G^{-1}, in (degrees)^2 for the solution 1, are listed in Table XII. From this, the standard deviations on the phase shifts are:

$$\alpha_1=-2.8°\pm4.5°,\ \alpha_3=-11.3°\pm3.2°,\ \alpha_{11}=-2.6°\pm7.5°,$$
$$\alpha_{13}=-2.1°\pm3.8°,\ \alpha_{31}=-11.6°\pm5.1°,\ \alpha_{33}=98.8°\pm3.6°.$$

In this determination of the errors in the phase shifts, all the experimental data have been used including the total cross sections from the transmission measurements. These errors are, however, only approximate, since the errors assigned to the cross sections are not independent and normally distributed, nor does M depend quadratically on the phase shifts.

The presence of D waves may introduce further uncertainties in the S and P phase shifts obtained above.[15] To test the possible effects of D wave phase shifts, Ashkin diagrams were drawn treating the D wave phase shift as a perturbation on the least squares values of $a+$, $b+$, and $c+$. With no D wave the solution was $\alpha_3=-13$, $\alpha_{33}=95°$, and $\alpha_{31}=-13°$; with the $T=\frac{3}{2}$ and $J=5/2$ D wave phase shift $\alpha_{35}=-5°$, the solution was only slightly different with $\alpha_3=-12$, $\alpha_{33}=96.5°$ and $\alpha_{31}=-12°$. The present data were not sufficiently accurate to warrant an explicit solution including D waves. Previous estimates by Henley and Ruderman[16] would yield $-2.8°$, Orear's estimate[15] would yield $-6.8°$ for α_{35}. However, the rapid fall of the total π^+ cross section above 200 Mev makes a sizeable D wave contribution seem unlikely.

DISCUSSION

Four sets of phase shifts have been found which fit the scattering data at 189 Mev. The data are fitted equally well if in any given set the signs of all the phase shifts are reversed. Moreover, it is always permissible to add 180° to any phase shift without altering the scattering amplitudes. Our solution 1 with signs reversed and 180° added to α_{33} corresponds quite closely to the choice preferred by de Hoffmann, Metropolis, Alei, and Bethe in their analysis of earlier scattering data.[2] Thus, our result is in agreement with their preferred solution, except that the present result would have α_{33} cross 90° at an energy somewhat less than 189 Mev. The phase shifts which correspond to solution 1 (resonance) are plotted in Fig. 8.

TABLE XII. Error matrix for phase shift solution 1 (degrees)^2.

	α_1	α_3	α_{11}	α_{13}	α_{31}	α_{33}
α_1	20.3	−6.84	− 7.01	− 5.15	7.32	− 2.16
α_3		9.93	2.18	0.791	− 3.92	− 0.957
α_{11}			56.7	−13.9	−14.3	1.59
α_{13}				14.6	− 2.74	1.33
α_{31}					25.7	− 8.66
α_{33}						13.2

[15] J. Orear, Phys. Rev. 98, 1155(A) (1955).
[16] E. M. Henley and M. Ruderman, Phys. Rev. 90, 719 (1953).

Recently Chew[17] has proposed a theory which gives a particularly simple behavior for α_{33}. In his model

$$\frac{k^3}{\omega_q^*}\cot\alpha_{33}=\frac{1}{\lambda_\alpha}\left(1-\frac{\omega_q^*}{\omega_{\text{res}}}\right)$$

where k is the momentum of the meson, ω_q^* is the total energy minus the proton rest mass, and λ_α is related to the coupling constant. The results of the scattering experiments are plotted according to this scheme in Fig. 9. It is seen that the agreement is remarkably good. A similar dependence is predicted for the other P wave phase shifts, except that the plot for these must have a slope opposite to that given for α_{33}. The experimental data are not inconsistent with this in view of the small values of α_{31}, α_{13}, and α_{11} in the preferred solution. However, the value $\alpha_{31}=236°$ from solution 2 with signs reversed would be hard to reconcile with Chew's theory.

The choice of solution 1 with signs reversed is also in agreement with requirements from causality. Karplus and Ruderman[18] and also Goldberger, Oehme, and Miyazawa[18] have derived dispersion relations based on the condition that signals cannot propagate faster than the speed of light. Through these, the real part of the forward scattering amplitude can be calculated from the knowledge of the total scattering cross sections for negative as well as positive pions by protons. These data now extend up to 1.9 Bev[19,20] and so permit a reliable evaluation of the dispersion integrals to be made. It is a striking result of this calculation that for the isotopic spin $\frac{3}{2}$ state the real part of the forward scattering amplitude changes sign abruptly between 165 Mev and 189 Mev. In terms of the phase shifts up to P waves the real part of the forward scattering amplitude is given by

$$\mathrm{R}(f_3)=(k_L/2k_b^2)(\sin2\alpha_3+2\sin2\alpha_{33}+\sin2\alpha_{31}),$$

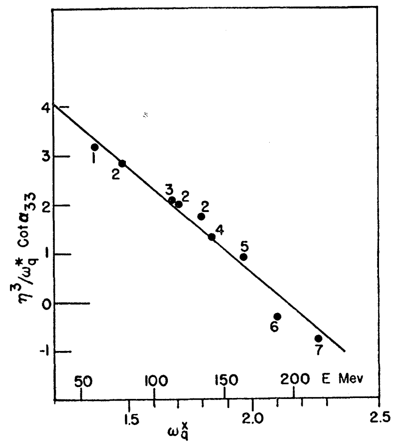

FIG. 9. Plot of $k^3/\omega_q^*\cot\alpha_{33}$ against ω_q^* for comparison to theory of G. Chew: R is the center of mass momentum of the pion, and ω_q^* is the center of mass energy minus the proton rest mass. 1. B. S. S., Columbia, reference 12; 2. A. F. M. and N., Chicago, reference 6; 3. Chicago, [J. Orear, Phys. Rev. **96**, 1417 (1954)]. 4. Washington University, J. J. Lord and A. B. Weaver (private communication). 5. A. and G., Chicago, reference 5; 6. A. D. G. and K., Chicago (present data); 7.Chicago, [M. Glicksman, Phys. Rev. **94**, 1335 (1954)].

where k_b and k_L are the wave numbers of the pions in the center of mass and laboratory systems, respectively.

The dispersion relations gave $\mathrm{R}(f_3)$ positive and in good agreement with the experimentally determined phase shifts below 180 Mev. Above 180 Mev, $\mathrm{R}(f_3)$ becomes abruptly negative in agreement with the phase shifts listed in Fig. 7 provided the phase shifts are taken with signs reversed. This makes solution 1 with signs reversed the solution of choice. Solutions 3 and 4 now have $\alpha_3=+44°$ and seem most unlikely in view of $\alpha_3=-20°$ or less at 165 Mev.[5] In solution 2, α_{33} goes over to 126° and α_{31} goes over to 236° implying rather large changes in two of the phase shifts. This seems unlikely on grounds of simplicity. Further details and other implications of these dispersion relations for the pion scattering will be published shortly.

ACKNOWLEDGMENTS

It is a pleasure to acknowledge the contributions of Joseph Fainberg and Tadao Fujii to the running of the equipment. We are grateful to Dr. Donald Flanders and Jean Hall of the Argonne National Laboratory for making available the AVIDAC for computing the phase-shift solutions.

[17] G. F. Chew, Fifth Annual Rochester Conference, 1955 (Interscience Publishers, Inc., New York, 1955).
[18] R. Karplus and M. Ruderman, Proceedings of Fifth Annual Rochester Conference, 1955 (Interscience Publishers, Inc., New York, 1955); Goldberger, Oehme, and Miyazawa, Phys. Rev. **99**, 986 (1955).
[19] Ashkin, Blaser, Feiner, Gorman, and Stern, Phys. Rev. **96**, 1104 (1954).
[20] S. J. Lindenbaum and L. C. Yuan; Cool, Clarke, and Piccioni, Fifth Annual Rochester Conference, 1955 (Interscience Publishers, Inc., New York, 1955).